Utilization of Solar Energy for Water Desalination and Purification Using Solar Concentrator

Pavel Navitski[1,*], *Jurabek* Izzatillaev[2], *Ali Al Taleb* Al Dor[1], *Ivan Samuel* Esley[1], *Jonathan* Merheb[1], *Lucas* Oliveira[1], and *Khaled A.* Sallam[3]

[1]School of Engineering, Oral Roberts University, Tulsa, OK, USA
[2]Department of Power Supply and Renewable Energy Sources, Tashkent Institute of Irrigation and Agricultural Mechanization Engineers National Research University, Tashkent, Uzbekistan
[3]Mechanical & Aero-Space Engineering, Oklahoma State University, Stillwater, OK, USA

Abstract. This paper focuses on a a solar energy-based project aimed at water desalination and purification. The project's objective is to establish an economically viable and sustainable approach to water heating and desalination, offering benefits to global communities. The project team has devised a solar heating system utilizing a Fresnel array-inspired setup, intended to complement a desalination system employing membrane distillation, which necessitates water heating. The primary focus has been on designing an efficient solar receiver to absorb solar energy for water heating. Moreover, the team has developed equations for concentrator mirror angles across various days, generating charts indicating optimal mirror angles and spacing between mirror rows for different solar times. Project outcomes involve applying heat transfer loss theory via conduction across individual receiver layers, conducting experiments to assess coating efficiency and receiver performance. The team successfully assembled the system with four parallel mirror rows, spaced at 1.5 feet intervals to minimize shadow casting. The solar receiver features two glass tubes, air gaps held by 3D-printed end caps, and an internal mesh turbulator to enhance heat transfer through flow turbulence. The ultimate objective was to heat water sufficiently for membrane distillation (around 40°-70°C). Experimental testing on a windy day with clouds resulted in a final water temperature of 38°C after 3 hours. Receiver efficiency, calculated by comparing solar energy incident on the pipe to energy transferred to water, was 17.5%. While not within the desired range, these promising results, considering surrounding conditions, deem the project successful in creating an efficient heating system for membrane distillation. Recommendations and improvements are possible, confirming the project as a successful proof of concept.

1. Introduction

The primary objective of this project is to construct an economical and reliable solar concentrator capable of heating impure water to temperatures ranging from approximately 40 to 70 degrees Celsius. This concentrator is intended to be integrated with a thermal desalination system that employs membrane distillation to eliminate impurities and salt from the water. Additionally, the project aims to create a scalable and easily reproducible design. In 2014, Oklahoma disposed of around 1.5 billion barrels of saline water underground, highlighting the need for utilizing such water resources [12]. The project also seeks to develop a cost-effective design applicable to third-world countries [1]. Also Results of the research can be used in the study process of engineers [15].

Currently, the project serves as a proof of concept, testing the feasibility of heating water within the specified temperature range using a compact and affordable flat plate Fresnel concentrator. The project's investigation consists of two main components: the concentrator and the receiver. The concentrator encompasses a framework with rows of flat mirrors designed to focus sunlight effectively, following a Fresnel Array or Linear Fresnel Reflector (LFR) design. Research demonstrates that LFRs offer unique advantages, such as reduced maintenance and operational costs compared to other solar concentration methods [13]. A sketch of a typical LFR can be seen in Figure 1 below.

* Corresponding author: pnavitski@oru.edu

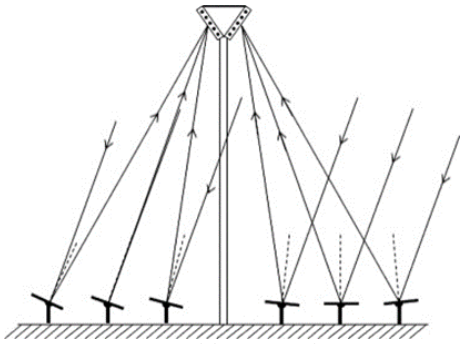

Fig. 1. LFR with two receivers [13]

Turning to the receiver design, similar concepts are utilized in solar cooker projects found in literature. The approach involves two glass tubes surrounding an inner pipe containing water, creating an air gap to trap heat. The inner glass tube is coated with a material possessing high absorptivity and low emissivity [9]. The integration of these systems is relatively uncommon, but similar projects using a motorized Fresnel array and vacuum tube for insulated cooking chambers have been documented [8].

Relevant patents include those related to vacuum tubes and solar cookers. Although patents like US9655469B2 and CN2112334 focus on specific portable cooker systems, they offer insights into vacuum tube usage. Additionally, JP2013228184A discusses advanced Fresnel Array designs [15].

Regarding standards, ASTM Standard A960/A960M-20 is relevant for internal piping in the receiver, while ASTM Standard for absorptive materials used in solar collectors guides coating selection [3, 4]. ASME standard STP-PT-054 analyzes concentrated solar power (CSP) designs, including Linear Fresnel Systems [2]. The data of performing research may be used in control algorithms and monitoring since computer control systems are widely used during multiple processes [7].

The project's technical aspects involve the concentrator and receiver designs. To maintain simplicity, a fixed mirror design without electronics is preferred. Among concentrator designs, a Fresnel flat-plate design was chosen due to its cost-effectiveness compared to complex parabolic designs. Challenges include determining optimal mirror angles for energy focus throughout the year. The receiver design aims to capture and retain maximum energy using two borosilicate glass tubes with an air gap, surrounding a smaller black pipe. Coating the inner glass tube enhances energy absorption and minimizes emission. Precise dimensions and end cap design are essential for success.

2. Engineering Analysis

To position the mirrors accurately, determining the sun's position in terms of altitude (α) and azimuth angles (β) is essential. The altitude angle depends on the declination (δ), found using the formula:

$\sin(\delta) = 0.39795 \cdot \cos[0.98563 \cdot (N - 173)]$, where

N represents the day of the year [16].

The hour angle (H) is calculated using:

$H = ((STh - 12) * 15)$, where

STh stands for solar time in hours.

Based on these values, the altitude angle is determined as:

$\alpha = sin{-}1(sin\varphi * sin\delta + cos\varphi * cos\delta * cosH)$, where

φ indicates the latitude.

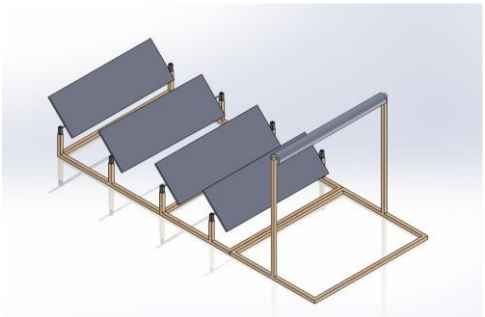

Fig. 2. SOLIDWORKS model of the concentrator

These angles define the sun's position at specific dates and times, leading to θ, the mirror angle, calculation using known mirror-to-pipe distance and height differences [16].
The project introduces an east-west configuration instead of the common north-south configuration. This configuration places all mirrors on the same side of the concentrator, enhancing efficiency. Figure 2 displays the SOLIDWORKS model of this design.
Efficient mirror positioning necessitates calculating shadow lengths cast by mirrors on different days of the year, ensuring rows aren't shadowed by those in front. Shadow lengths (SL) are determined by mirror height (MH) [14].
Design constraints encompass ease of transport, a 4-ft receiver length for desired water output (40-70°C), use of 4 mirror rows, 1.5-ft spacing, easy assembly, affordability, and Dr. Sallam's guidance.
Mirror angles are derived using the equation presented in Figure 3.

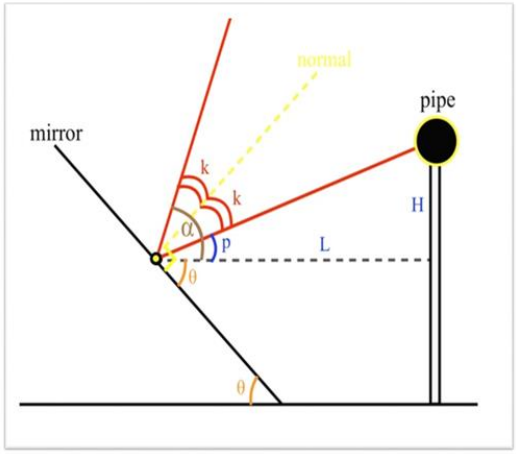

Fig. 3. Mirror Angle Diagram

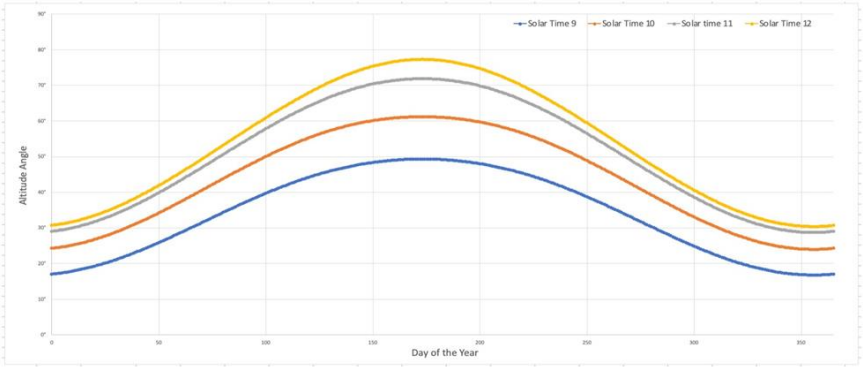

Fig. 4. Solar altitude angle variation throughout the year for constant solar times

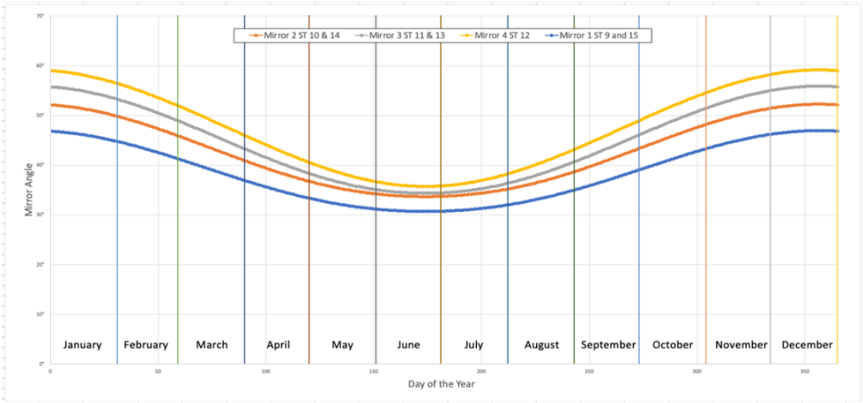

Fig. 5. Plot of mirror angle variation throughout the year

Calculated angles are tabulated for different months. Solar altitude angle variation across the year (for constant solar times) is shown in Figure 4. Mirror angles for various solar times (9, 10, 11, and 12) are plotted throughout the year in Figure 5. These calculations and graphs are generated using an Excel spreadsheet.
Data from the spreadsheet facilitates creating a chart depicting different mirror angles for various months, as displayed in Table 1. This aids in mirror positioning for optimal solar concentration.

Table 1. Updated mirror angle chart for solar time 12

	Mirror 1	Mirror 2	Mirror 3	Mirror 4
January	46°	51°	55°	58°
February	43°	48°	51°	54°
March	39°	43°	46°	49°
April	35°	39°	40°	43°
May	32°	35°	36°	38°
June	31°	34°	35°	36°
July	31°	34°	35°	37°
August	34°	37°	39°	41°
September	37°	41°	44°	46°
October	41°	46°	49°	52°
November	45°	50°	54°	57°
December	47°	52°	56°	59°

The chart shown earlier involves assigning angles to each mirror, with the mirror closest to the pipe (mirror 1) receiving angles for the smallest solar time (9 or 15). This approach acknowledges that early and late in the day, the sun casts larger shadows, potentially affecting rear mirrors more. Mirror 2 gets angles for solar time 10 (and 14), mirror 3 for solar time 11 (and 13), and mirror 4 for solar time 12. The mirror angles increase as the mirror moves away from the pipe. Notably, the mirror angles remain quite consistent within a given month. This suggests that multiple mirrors are likely to contribute to focusing sunlight on the pipe simultaneously due to the mirror height (1ft) being larger than the pipe's diameter, allowing for some margin of error. A column chart displaying average mirror angles for different months throughout the year further illustrates this (Figure 6).

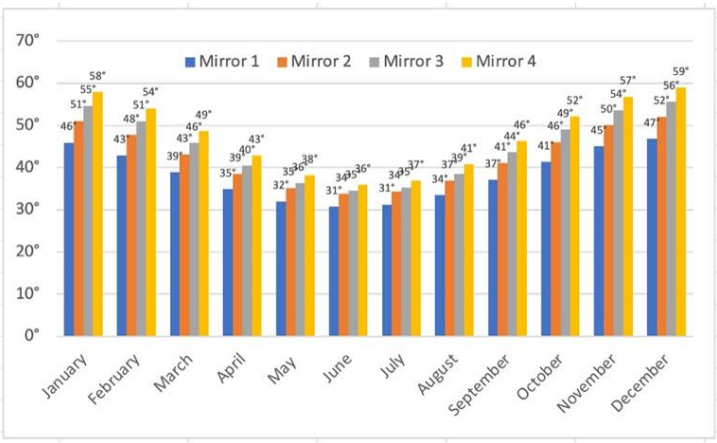

Fig. 6. Mirror angle variation in column chart format

Table 2: Updated mirror angle chart for solar time 12

	Mirror 1	Mirror 2	Mirror 3	Mirror 4
January	39°	48°	54°	58°
February	35°	44°	50°	54°
March	30°	39°	45°	49°
April	24°	33°	39°	43°
May	19°	28°	34°	38°
June	17°	26°	32°	36°
July	18°	27°	33°	37°
August	22°	31°	37°	41°
September	27°	36°	42°	46°
October	33°	42°	48°	52°
November	38°	47°	53°	57°
December	40°	49°	55°	59°

Upon testing, the group discovered that leaving the frame stationary during active times (solar time 10 to solar time 14) was inefficient. Instead, turning the concentrator hourly or half-hourly to face the sun's direction proved more effective, maximizing mirror reflection on the receiver. Consequently, the mirror angle chart was adapted to include a chart for every solar time. Table 2 depict the mirror angle plot and updated chart for solar time 12 as an example.
Considering the optimal receiver design involves evaluating the effectiveness of utilizing one glass tube, two glass tubes, or no glass tubes.
Calculations for a single glass tube's heat transfer necessitate certain assumptions. It is assumed that the insulating air gap experiences minimal convection, relying primarily on conduction due to its small size. Furthermore, the water in the pipe is assumed to be at 70°C, while ambient air temperature is set at 25°C, and heat loss results from natural convection of ambient air.
Heat loss in Watts can be calculated using an equation that factors in water pipe temperature, ambient air temperature, and total thermal resistance in °C/W [5].
Calculating thermal resistance entails considering all layers involved in heat transfer. This encompasses convection through the water in the pipe, conduction through the pipe, air, and glass, and convection due to ambient air. However, using two glass tubes yields significantly more promising outcomes.
Comparatively, the absence of glass tubes results in the following heat loss. Hence, employing two glass tubes leads to substantial improvements in minimizing heat loss, offering nearly three times the efficacy of a single glass tube. This becomes the chosen design. However, it's worth noting that while adding more glass tubes further reduces energy loss, the incremental benefits diminish. The project adheres to the law of diminishing returns, as more glass tubes would escalate costs without proportional benefits.
For precision and adherence to advisor and theoretical constraints, SOLIDWORKS models and drawings are created. The end cap design, accommodates the black pipe through the centered hole while the inner and outer glass tubes rest atop the end cap's cut extrusions. The entire end cap measures 2 inches in length. The initial receiver design, was bulkier and incorporated heat pipes and larger air gaps, potentially undermining the anti-heat loss concept. The design was subsequently refined, considering accuracy and replicability, resulting in the final receiver design showcased in Figure 7.

Fig. 7. Final receiver design

In terms of glass selection, borosilicate glass was chosen for its durability, affordability, and low coefficient of thermal expansion, making it resilient to high-heat conditions. To enhance heat transfer to the water within the receiver, a mesh turbulator was employed. The mesh turbulator disrupts the boundary layer, augmenting heat transfer from the pipe to the water.

3. Experimental Measurements and Testing

The initial phase of testing conducted in this project played a pivotal role in shaping the device's design process. Solar is one of the renewable energy sources along with the biogas, hydro, thermal etc. with high potential [10] without environmental pollution [11]. The focus was on the receiver's design, particularly on optimizing heat transfer and solar energy retention on the steel pipe via radiation. A strategy to enhance this involved coating the pipe with a substance featuring high absorptivity and low emissivity. The coating was aimed at retaining heat and gradually elevating the pipe's temperature. After weighing factors like cost and absorptivity, the chosen coating was a High Temperature Silicone Coating—commonly used in industries like automotive manufacturing. To verify its effectiveness, the coating underwent testing against a control pipe, marking the project's inaugural experiment.
One pipe remained untreated as the control, while the other received three layers of the high-temperature silicone coating. The objective was to simulate heat transfer from the sun into water through the piping. To simulate this scenario, both experimental pipes were sealed at one end and filled with an equal volume of water. Placed side by

side in direct sunlight, mercury thermometers within the water gauged temperature changes. The temperatures were monitored over 9 intervals spanning 100 minutes to allow adequate observation of the coating's impact. The data was tabulated and is presented in Table 3.

Table 3. Coating data

Time	Not Coated (°C)	Coated (°C)
3:00 PM	24	24
3:10 PM	27	29
3:20 PM	28.5	30
3:30 PM	29	30
3:40 PM	29	30.5
3:50 PM	28.5	30
4:00 PM	28	29.5
4:20 PM	28	29.5
4:40 PM	27.5	29

For a clearer visual representation of the data, a graph was plotted to compare the coated and non-coated pipes concurrently. This graph is depicted in Figure 8.

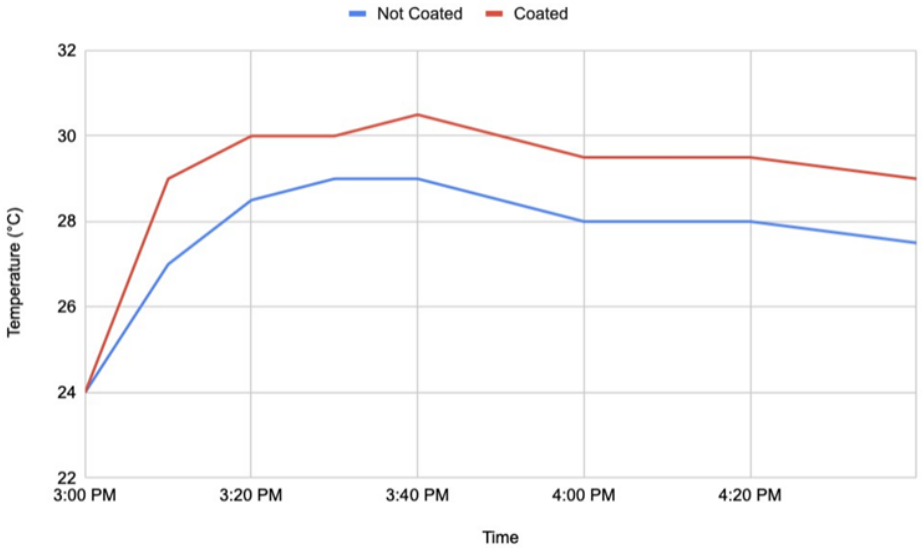

Fig. 8. Coating versus no coating comparison

Upon analyzing this data, it's possible to draw conclusions about the coating's effectiveness. The results indicate that the coating indeed aided in retaining solar energy, maintaining consistently higher temperatures in the coated pipe compared to the control pipe. Throughout the experiment, the average temperature difference of roughly 2°C encouraged the coating's use in the final design, as it corroborated the initial hypothesis. Although the temperature variance might not be significant, the observation that treatment outperformed the untreated control validated the concept. It's important to recognize that the experiment took place in early spring with relatively low solar irradiation and strong winds. As such, the coating's efficacy could potentially prove even more compelling on sunnier days during summer.

The subsequent testing phase centered on evaluating the fully assembled concentrator's effectiveness. The goal was to gauge the system's efficiency in heating water. This was accomplished by measuring temperature increases over time as water passed through the concentrator. To begin, the water volume under examination had to be established. A bucket contained the water, and its volume was determined by measuring its diameter and depth with a tape measure, then calculating the cylinder's volume with those measurements.

Subsequently, the initial water temperature was noted, and the system was activated. Employing an east-west configuration (receiver in the east-west plane) required all mirrors to be positioned on one side. The concentrator was aligned with the sun, its orientation changed every 30 minutes to maintain alignment. The mirrors concentrated sunlight onto the receivers. A solar-powered pump circulated water from the bucket through the receiver and back.

To eliminate external heating influences, cardboard covered the bucket throughout the experiment, focusing on observing the receiver's heating effects. This setup is displayed in Figure 9.

Fig. 9. Concentrator and receiver configuration for testing

The experiment aimed to ascertain the water's temperature change over the observed timeframe. For the preliminary system test, measurements were conducted between 0 and 120 minutes, with temperatures ranging from 20 to 35°C. The results demonstrated the system's ability to transfer heat to the water, in line with expectations, with a temperature difference (ΔT) of 15°C. However, the experiment also underscored the system's susceptibility to external factors like clouds and wind. The final temperature after 2 hours of testing fell below expectations due to relatively low solar irradiance. Subsequent testing under similar weather conditions served as the project's conclusive round. The data from this final test, conducted between 0 and 190 minutes, with temperatures ranging from 19 to 38°C, indicated a more promising temperature difference (ΔT) of 19°C. The final temperature of 38°C was closer to the target range of 40-70°C, optimal for effective membrane distillation.

4. Project Validation

At the start of the semester, the team aimed for a design that could attain 70°C temperatures, deeming it a measure of completeness. As the university semester terms were mildly changed after COVID period it became more appropriate to do it [6]. As testing progressed, it became apparent that this goal was impractical, especially beyond summer's warmth. Thus, the completeness criteria evolved to encompass water temperatures from 40°C to 70°C.

To validate the design's accomplishment of this temperature range, the final prototype adhered to the above-discussed theory and calculations. Tests were conducted, resulting in a peak temperature of 38°C. While not precisely within the desired range, achieving this in summertime seems feasible. Hence, the group deems the project complete. However, it's worth noting that efficiency-enhancing modifications are possible, outlined in the recommendations section.

5. Results

To thoroughly validate the effectiveness and viability of the concentrator and receiver design, the team conducted both a preliminary and a final test. The preliminary test took place on a relatively windy day with an ambient temperature of around 23°C and a water volume of 3 US gallons. This initial experiment yielded a ΔT of 15°C over a 2-hour testing period. To further substantiate these findings and extend the testing duration, a final test was conducted under similar conditions, again on a windy day with an ambient temperature of approximately 23°C. This time, a water volume of 1.65 US gallons was utilized. The data from the final test was organized into a graph, as shown in Figure 10.

The graph indicates a ΔT of 19°C over slightly more than 3 hours. It is assumed that the water reaches an energy equilibrium point, where the energy gained equals the energy lost, leading to a relatively plateaued temperature change between 120 and 180 minutes.

Although the final temperature isn't precisely within the intended range, the team still considers the project complete and its objectives validated. The testing conditions, characterized by windy days, led to enhanced cooling due to forced convection, influencing the results more than on calmer days. The team anticipates that during warmer summer days, temperatures can easily reach the desired 40°C to 70°C range for effective desalination. Even at the current 38°C, the desalination system is likely to function. While this falls on the lower end of the range, the system could manage by supplying slightly higher pressure on the desalination end, which the team's identified solar pump seems well-equipped to handle.

With a receiver efficiency of 17.5%, the team is content. This efficiency level compares favorably with that of most solar panels, which typically range from 15% to 20%. While recognizing the differences between the systems, this

perspective highlights the respectable performance of the solar energy utilization. Future enhancements to the design could potentially contribute to boosting the project's overall efficiency.

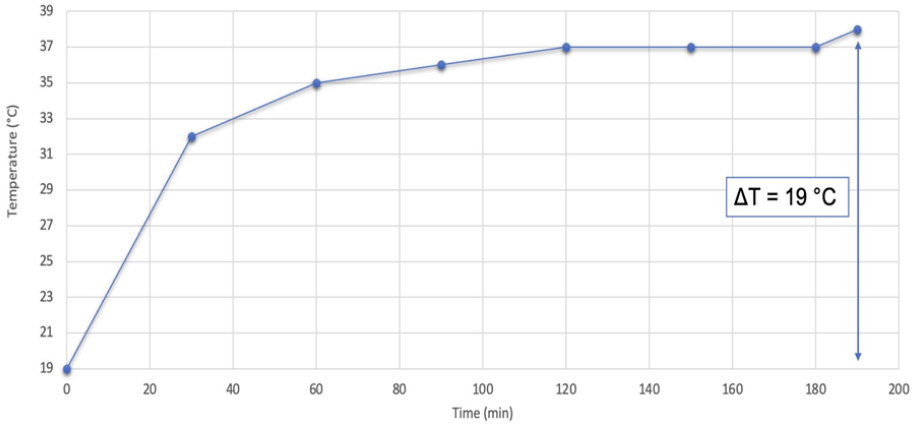

Fig. 10. Final test data plot

6. Conclusions and Recommendations

In conclusion, the team finds the final outcomes of this project to be satisfactory. While the exact 40°C to 70°C range was not achieved, attaining a final temperature of 38°C is deemed a success. With warmer days and reduced wind-driven convection, it's anticipated that the water temperature will readily fall within the desired range, lending support to the theoretical foundation and showcasing the design's potential.

Results of the research can be used in the study process of engineers.

Several recommendations are put forth to enhance this design further. To begin, extending the length of the end caps beyond 2 inches is advised. Movement of the frame caused some glass cracking at one end, and longer end caps could distribute weight more effectively. Enlarging the openings where the glass rests can alleviate glass tension. Air-tight seals could be formed using O-rings, potentially reducing heat transfer from the black pipe.

For future iterations, consideration should be given to crafting end caps from more durable materials. During testing, the end caps began to melt due to intense heat exposure. Opting for lightweight metal or plexiglass could bolster durability in high-heat and sunlight environments. Addressing heat loss at the extremities of the black pipe by utilizing shorter pipes or extended glass tubes would contribute to minimizing energy loss and optimizing energy transfer to the water.

Ultimately, integrating a mechanism for easy adjustment throughout the day is strongly recommended. This could involve motorized automation or manual addition of all-terrain wheels to each compartment. Leaving the design stationary on a sunny day is inefficient, as the solar receiver is fully covered by sunlight only at a specific solar time. To maximize efficiency, continuous alignment with the sun is crucial. Alternatively, a north-south configuration may prove superior to the east-west configuration used in this project.

References

1. Jurabek Izzatillaev, Pavel Navitski, Sirojiddin Khushiev, Abdushoxid Mamadjanov, and Azizbek Akrombaev Determination of technical and economic efficiency of microgrid based on renewable energy sources. 2nd International Conference on Energetics, Civil and Agricultural Engineering 2021 (ICECAE 2021) AIP Conf. Proc. 2686, 020017-1–020017-7; https://doi.org/10.1063/5.0119115
2. ASME 2012 “STP-Pt-054 - 2012 CSP Codes & Standards Gap Analysis.” ASME, https://www.asme.org/codes-standards/find-codes-standards/stp-pt-054-concentrated-sola r-power-codes-standards-gap-analysis/2012/drm-enabled-pdf.
3. ASTM 2020 “Standard Specification for Common Requirements for Wrought Steel Piping Fittings.” ASTM International - Standards Worldwide, https://www.astm.org/a0960_a0960m-20.html.
4. ASTM 2022 “Standard Practice for Evaluating Solar Absorptive Materials for Thermal Applications.” ASTM International - Standards Worldwide, https://www.astm.org/e0744-07r22.html.
5. Baukal, Charles. “Heat Transfer 2023-01-30 Chapter 03 Steady Heat Conduction 2.” D2L ORU.
6. Navitski P., Gregg E. Physics teaching at Oral Roberts University during the pandemic time. Proceedings of the VII International Scientific Conference "Digital Education at Environmental Universities—Dnipro: Serednyak TK, 2021, p. 20-21.

7. Клочков, А. В., Новицкий, П. М., Ковалев, В. Г., & Гусаров, В. В. Электронные системы и устройства сельскохозяйственных машин. Учебное пособие для студентов учреждений высшего образования по специальности "Техническое обеспечение процессов сельскохозяйственного производства" / Минск, 2019.
8. Farooqui, S. Z. (2013). A vacuum tube based improved solar cooker. Sustainable Energy Technologies and Assessments, 3, 33–39. https://doi.org/10.1016/j.seta.2013.05.004
9. Hosseinzadeh, Mohammad, et al. “Parametric Analysis and Optimization of a Portable Evacuated Tube Solar Cooker.” Energy, vol. 194, 2020, p. 116816., https://doi.org/10.1016/j.energy.2019.116816.
10. Клочков А. В., Новицкий П. М. Биогаз: итоги и перспективы использования //Наше сельское хозяйство. – 2017. – №. 74. – С. 34-35.
11. Navitski P., Ruckelshausen A. Ecological monitoring of pesticide drift of machines for chemical plant protection in the republic of Belarus using sensors technologies. Proceedings of the V International conference: “Digital Education at Environmental Universities”, 17-18 October 2018, National University of Life and Environmental Sciences of Ukraine, Kyiv, Ukraine, 2018. – pp. 118-121
12. Oklahoma Water Resources Board | The Water Agency. (n.d.). Retrieved November 12, 2022.
13. R. Abbas, et al. Solar Radiation Concentration Features in Linear Fresnel Reflector Arrays. Energy Conversion and Management, vol. 54, no. 1, 2012, pp. 133–144., https://doi.org/10.1016/j.enconman.2011.10.010.
14. Sandnes, Frode Eika. “Determining the Geographical Location of Image Scenes Based on Object Shadow Lengths - Journal of Signal Processing Systems.” SpringerLink, Springer US, 5 Oct. 2010.
15. Navitski P. et al. Mechatronics teaching in preparing agricultural engineers for precision farming technology development //Theoretical and Applied Mechanics: International Scientific and Technical Journal. – 2015.
16. Yang, Chao-Kai, et al. “Open-Loop Altitude-Azimuth Concentrated Solar Tracking System for Solar-Thermal Applications.” Solar Energy, Pergamon, 19 Mar. 2017.